

ORIGINAL ARTICLE

## Effect of retinal ischemia on the non-image forming visual system

María Florencia González Fleitas\*, Melina Bordone\*, Ruth E. Rosenstein, and Damián Dorfman

*Laboratorio de Neuroquímica Retiniana y Oftalmología Experimental, Departamento de Bioquímica Humana, Facultad de Medicina/CEfyBO, Universidad de Buenos Aires/CONICET, Buenos Aires, Argentina*

Retinal ischemic injury is an important cause of visual impairment. The loss of retinal ganglion cells (RGCs) is a key sign of retinal ischemic damage. A subset of RGCs expressing the photopigment melanopsin (mRGCs) regulates non-image-forming visual functions such as the pupillary light reflex (PLR), and circadian rhythms. We studied the effect of retinal ischemia on mRGCs and the non-image-forming visual system function. For this purpose, transient ischemia was induced by raising intraocular pressure to 120 mm Hg for 40 min followed by retinal reperfusion by restoring normal pressure. At 4 weeks post-treatment, animals were subjected to electroretinography and histological analysis. Ischemia induced a significant retinal dysfunction and histological alterations. At this time point, a significant decrease in the number of Brn3a(+) RGCs and in the anterograde transport from the retina to the superior colliculus and lateral geniculate nucleus was observed, whereas no differences in the number of mRGCs, melanopsin levels, and retinal projections to the suprachiasmatic nuclei and the olivary pretectal nucleus were detected. At low light intensity, a decrease in pupil constriction was observed in intact eyes contralateral to ischemic eyes, whereas at high light intensity, retinal ischemia did not affect the consensual PLR. Animals with ischemia in both eyes showed a conserved locomotor activity rhythm and a photoentrainment rate which did not differ from control animals. These results suggest that the non-image forming visual system was protected against retinal ischemic damage.

**Keywords:** Ischemia, melanopsin, non-image forming visual system, retina

### INTRODUCTION

Retinal ischemia is a significant contributor to major retinal diseases, such as glaucoma, diabetic retinopathy, and retinal and choroidal vessel occlusions, which lead to irreversible blindness (Bresnick et al., 1975; Kuehn et al., 2005; Osborne et al., 2004; Quaranta et al., 2013). During retinal ischemia, energy metabolism is halted, triggering a complex event cascade including free radical formation (Bonne et al., 1998), mitochondrial dysfunction (Liu et al., 2009), and glutamate excitotoxicity (Fernandez et al. 2009; Szydlowska & Tymianski, 2010), which ultimately leads to cell death (reviewed by Osborne et al., 2004). In addition to ischemic damage, the process of reperfusion itself is deleterious to injured cells with the potential to aggravate ischemic damage, an effect known as reperfusion injury.

Retinal ganglion cells (RGC) appear to be particularly susceptible to ischemic cell death (Chidlow & Osborne, 2003; Lafuente et al., 2002). A subset of RGCs which express the photopigment melanopsin (mRGCs) are intrinsically photosensitive, and drive

non-image-forming visual functions, including light-driven circadian and sleep behaviors and the pupillary light reflex (PLR). Intrinsically, photosensitive RGC express melanopsin, an opsin that responds directly to light (Berson et al., 2002; Hankins et al., 2008; Hattar et al., 2002, 2003; Lucas et al., 2001; Panda et al., 2003; Provencio et al., 2002). Intrinsically photosensitive RGCs that drive the circadian rhythm project mainly to the suprachiasmatic nucleus (SCN) (Berson et al., 2002; Gooley et al., 2001), while those that are responsible for the PLR project to the olivary pretectal nucleus (OPN) and intergeniculate leaflet (reviewed by Berson, 2003). Since the photic information plays a key role in the generation of biological rhythms (Guido et al., 2010), it is of great interest to determine how retinal diseases may affect the circadian timing system.

Much research has been devoted to describing visual dysfunction and RGC loss in retinal ischemia; however, the influence of retinal ischemia on the non-image-forming visual system has not been previously investigated. Considering that ischemic insult to

Submitted July 10, 2014, Returned for revision August 19, 2014, Accepted August 26, 2014

\*María Florencia González Fleitas and Melina Bordone contributed equally to this work.

Correspondence: Dr. Ruth E. Rosenstein, Laboratorio de Neuroquímica Retiniana y Oftalmología Experimental, Departamento de Bioquímica Humana, Facultad de Medicina, CEFyBO, Paraguay 2155, 5°P, (1121), Universidad de Buenos Aires, CONICET, Buenos Aires, Argentina. Tel: 54-11-4508-3672 (ext. 37). Fax: 54-11-4508-3672 (ext. 31). E-mail: ruthr@fmed.uba.ar

the retina is associated with various prevalent retinal disorders, we considered it worthwhile to analyze the effect of retinal ischemia on mRGCs and the non-image-forming visual system.

## MATERIALS AND METHODS

### Animals

Adult male Wistar rats (average weight,  $250 \pm 50$  g) were housed in a standard animal room with food and water *ad libitum*, under controlled conditions of humidity and temperature ( $21 \pm 2^\circ\text{C}$ ). The room was lighted by fluorescent lights (200 lux) that were turned on and off automatically every 12 hours (on from 8.00 AM to 8.00 PM). A total of 40 animals were used, as follows: 10 animals in which one eye was submitted to retinal ischemia and the contralateral eye was subjected to a sham procedure were used for electroretinogram (ERG) recording of which 5 were used for histological studies, and 5 animals for anterograde transport studies; 20 animals in which one eye was submitted to sham procedure or ischemia whereas the contralateral eye remained intact were used for PLR assessment, of which 10 animals were used for immunohistochemistry, and 10 animals for Western blotting. In addition, 5 animals with bilateral ischemia, and 5 animals with sham procedure in both eyes were also used for locomotor activity studies. The ethics committee of the University of Buenos Aires School of Medicine, (Institutional Committee for the Care and Use of Laboratory Animals, (CICUAL)) approved this study which agrees with ARVO Statement for the Use of Animals in Ophthalmic and Vision Research. The experimental protocol conformed to international ethical standards (Portaluppi et al., 2010).

### Retinal ischemia

Animals were anesthetized with ketamine hydrochloride (150 mg/kg) and xylazine hydrochloride (2 mg/kg) administered intraperitoneally. After topical instillation of 0.5% proparacaine (Anestalcon, Alcon Laboratories, Buenos Aires, Argentina), the anterior chamber was cannulated with a 30-gauge needle connected to a pressurized bottle filled with sterile normal saline solution. Retinal ischemia was induced by increasing intraocular pressure to 120 mm Hg for exactly 40 min, while for the sham procedure, eyes were cannulated without raising IOP, as previously described (Dorfman et al., 2013; Fernandez et al., 2009). With this maneuver, complete ocular ischemia was produced, characterized by cessation of flow in retinal vessels, determined by fundusoscopic examination. In some experiments, animals were submitted to unilateral ischemia, while the contralateral eye was submitted to the sham procedure. In another set of experiments, ischemia was bilaterally induced and control animals were bilaterally submitted to the sham procedure. In the present

study, eyes submitted to a sham procedure served as the control group because in preliminary studies we found that in comparison with intact animals, this maneuver *per se* did not affect retinal function and histology (data not shown).

### Electroretinography

Electroretinographic activity was assessed at 4 weeks after ischemia, as previously described (Dorfman et al., 2013; Fernandez et al., 2009). Briefly, after 6 h of dark adaptation, rats were anesthetized under dim red illumination. Phenylephrine hydrochloride (5%) and tropicamide (0.5%) (Tropioftal F, Denver Farma, Buenos Aires, Argentina) were used to dilate the pupils, and the cornea was intermittently irrigated with balanced salt solution to maintain the baseline recording and to prevent keratopathy. Rats were placed facing the stimulus at a distance of 20 cm. All recordings were completed within 20 min. A reference electrode was placed through the ear, a grounding electrode was attached to the tail, and a gold electrode was placed in contact with the central cornea. A 15 W red light was used to enable accurate electrode placement. This maneuver did not significantly affect dark adaptation and was switched off during the electrophysiological recordings. Scotopic ERGs were recorded from both eyes simultaneously and 10 responses to flashes of unattenuated white light (5 ms, 0.2 Hz) from a photic stimulator (light-emitting diodes) set at maximum brightness were amplified (9 cd s/m<sup>2</sup> without filter), filtered (1.5-Hz low-pass filter, 1000 high-pass filter, notch activated) and averaged (Akonic BIO-PC, Buenos Aires, Argentina). The a-wave and b-wave amplitude and latency were assessed as previously described (Dorfman et al., 2013; Fernandez et al., 2009). To confirm consistency, ERGs were recorded 3 times with 5 min-intervals, and the results were averaged. Oscillatory potentials (OPs) were assessed as previously described (Dorfman et al., 2013; Fernandez et al., 2009). Briefly, the same photic stimulator with a 0.2 Hz frequency and filters of high (300 Hz) or low (100 Hz) frequency were used. The OP amplitudes were estimated by measuring the heights from the baseline drawn between the troughs of successive wavelets to their peaks. The sum of three OPs was used for statistical analysis.

### Retinal histology

Four weeks after ischemia, rats were anesthetized and intracardially perfused with saline solution, followed by a fixative solution containing 4% paraformaldehyde in 0.1 mol/L phosphate buffered saline (PBS) (pH 7.4). Then, the eyeballs and the brain were carefully removed and immersed for 24 h in the same fixative. After dehydration, eyes were embedded in paraffin wax and sectioned (5  $\mu\text{m}$ ) through the optic nerve head. Microscopic images were digitally captured with a microscope (Eclipse E400, Nikon, Tokyo, Japan); 6-V

halogen lamp, 20W, equipped with a stabilized light source and a camera (Coolpix s10; Nikon; Abingdon, VA, USA). Retinal sections were stained with hematoxylin and eosin, and analyzed by masked observers. The average thickness (in  $\mu\text{m}$ ) of the total retina was measured for each eye. Measurements were obtained at 1 mm dorsal and ventral from the optic disc. The number of cells in the ganglion cell layer (GCL) was counted along the whole retina section. For each eye, four separate sections were obtained with a microtome (Leica Biosystems, Buenos Aires, Argentina). The total retinal thickness and the number of RGC from each sample were averaged, and the mean of 5 eyes was recorded as the representative value for each group.

### Cholera toxin $\beta$ -subunit transport studies

Rats were anesthetized, and a drop of 0.5% proparacaine was topically administered for local anaesthesia. Using a 30-gauge Hamilton syringe (Hamilton, Reno, NV, USA), 4 microliters of a solution of 0.2% cholera toxin  $\beta$ -subunit (CTB) conjugated to Alexa 488 (green, Molecular Probes Inc., Eugene, OR) in 0.1 mol/L PBS (pH 7.4) were injected into the vitreous from an eye submitted to a sham procedure, and the same amount of 0.2% CTB conjugated to Alexa 594 (red, Molecular Probes Inc., Eugene, OR) was injected in the vitreous from the contralateral ischemic eye. The injections were applied 1 mm from the limbus, and the needle was left in the eye for 30 seconds to prevent volume loss. Three days after injection, rats were anesthetized and intracardially perfused. Brains were carefully removed, post-fixed overnight at 4°C, and immersed in a graded series of sucrose solutions for cryoprotection; coronal sections (40  $\mu\text{m}$ ) were obtained using a freezing microtome (Leica Biosystems, Buenos Aires, Argentina). Sections from superior colliculus (SC), lateral geniculate nuclei (LGN), suprachiasmatic nuclei (SCN), and olivary pretectal nuclei (OPN) were obtained. Sections were mounted with antifade medium (Dako, Glostrup, Denmark) and viewed under an epifluorescence microscope, as previously described (Dorfman et al., 2013).

### Morphometric analysis

All the images were assembled and processed using Adobe Photoshop SC (Adobe Systems, San Jose, CA) to adjust the brightness and contrast. No other adjustments were made. For all morphometric image processing and analysis, digitalized captured TIFF images were transferred to ImageJ software version 1.42q (NIH, Bethesda, MD). All the nomenclature used herein follows that one of Paxinos & Watson (1997).

### RGC studies

Four weeks after ischemia, animals were intracardially perfused as previously stated. Eyeballs were carefully removed and corneas and lens were cut off. Eye-cups were post-fixed in 4% paraformaldehyde in 0.1 mol/L PBS (pH 7.4) for 30 min. Whole-mount retinas were

obtained and oriented. After several washes in PBS, retinas were immersed in 0.1 mol/L PBS containing 0.1% Triton X-100, for 20 min, and then pre-incubated with equine serum 0.2% in PBS overnight for unspecific blockade. Retinas were then incubated with a goat anti-Brn3a antibody (1:500; Santa Cruz Biotechnology, Inc., Dallas, TX), and a rabbit polyclonal anti-melanopsin (1:750, Affinity Bioreagent, Rockford, IL) for 48 h. After several washes, retinas were incubated with a goat anti-rabbit secondary antibody conjugated to Alexa 488 (1:500; Invitrogen, Molecular Probes) and a donkey anti-goat secondary antibody conjugated to Alexa 568 (1:500; Invitrogen, Molecular Probes, Grand Island, NY) for 2 h at room temperature. Finally, retinas were mounted with fluorescent mounting medium (Dako, Rochem Biocare, Buenos Aires, Argentina) and observed under an epifluorescence microscope (BX50; Olympus, Tokyo, Japan) connected to a video camera (3CCD; Sony, Tokyo, Japan) attached to a computer running image analysis software (Image-Pro Plus; Media Cybernetics Inc., Bethesda, MD). Complete retinal reconstructions were achieved combining digital images obtained at low magnification with identical exposure time, brightness, and contrast settings using Adobe Photoshop SC (Adobe Systems, San Jose, CA). The total area of the retina was calculated using ImageJ software (NIH, USA).

To determine the number of RGCs, retinas were divided into four quadrants. Digital images (area corresponding to 0.1 mm<sup>2</sup>) from each quadrant were obtained (200 $\times$ ). Images were converted to 8-bit gray scale and the number of Brn3a(+) cells were counted using ImageJ software (NIH, USA). The average of 20 images was recorded for each retina and was expressed as the number of Brn3a(+) cells in 2 mm<sup>2</sup>. For each group, the mean of five retinas was recorded as the representative value. The number of melanopsin(+) cells was determined. For each digitally reconstructed retina, the total number of cells was manually counted. Finally, a schematic drawing of the immune-stained retinas was obtained. For each group, the mean of five eyes was recorded as the representative value.

### Western blotting

Retinas were homogenized in 100  $\mu\text{L}$  of a buffer containing 10 mM HEPES, 1 mM EDTA, 1 mM EGTA, 10 mM KCl, 0.5% (v/v) Triton, pH 7.9, supplemented with a cocktail of protease inhibitors (Sigma Chemical Co., St Louis, MO). After 15 min at 4°C, homogenates were gently vortexed for 15 s and centrifuged at 900  $\times$  g for 10 min. Supernatants were used to determine protein concentration. Proteins (100  $\mu\text{g}$ /sample) were separated in SDS, 12% PAGE. After electrophoresis, proteins were transferred to polyvinylidene difluoride membranes for 60 min at 15-V in a Bio-Rad Trans-Blot SD system (Bio-Rad Laboratories, Hercules, CA). Membranes were blocked in 3% BSA in Tris-buffered saline (pH 7.4) containing 0.1% Tween-20 for 60 min at room temperature and then incubated overnight at 4°C



with a rabbit polyclonal anti-melanopsin antibody (1:1000) and a goat polyclonal anti-Brn3a antibody (1:500). Membranes were washed and then incubated for 1 h with a horseradish peroxidase-conjugated secondary antibody. Immunoblots were visualized by enhanced chemiluminescence Western blotting detection reagents (Amersham Biosciences, Buenos Aires, Argentina). Autoradiographical signals were quantified by densitometry using ImageQuant software and adjusted by the density of  $\beta$ -actin. For each group, the mean of 10 retinas were recorded as the representative value. Protein content was determined by the method of Lowry et al. (1951), using BSA as the standard.

### Assessment of the pupil light reflex

Consensual PLR was assessed in dark-adapted animals for 2 h. For this purpose, light from a dim white light source (120 lux) was applied to one eye, while the other eye was video-monitored under infrared light with a digital camcorder (Sony DCR-SR60, Tokyo, Japan). After dark-adapting the animals for another 2 h, the same procedure was repeated with a bright white light (1200 lux). Sampling rate was 30 images per s. The digital video recording was deconstructed to individual frames using OSS Video Decompiler Software (One Stop Soft, New England, MA). The PLR was expressed as the percent of pupil area at 30 s after the initiation of the stimulus (steady state) relative to the dilated pupil size.

### Locomotor activity rhythm

Circadian rhythms of locomotor activity were registered under 12 h light (200 lux)/12 h dark cycles, as previously described (Fernandez et al., 2013). Animals were submitted to a bilateral sham procedure (control) or bilateral ischemia (ischemia) and after recovery from anesthesia were placed in cages equipped with infrared detectors of motion. Data were sampled every 5 min and stored for subsequent analysis during 40 d. Double-plot actograms, periodograms and average activity waveforms were built with El Temps software (A. Díez-Noguera, Barcelona, Spain). The phase angle for activity onset (with respect to the time of lights off) was determined, defined as the first of 5-min activity bins in which locomotor activity was higher than the average value of the diurnal waveform. In addition, the percentage of locomotor activity during the light and dark phases was computed. Re-entrainment rates were calculated after 4 h of phase delay in the light/dark (L:D) cycle, starting by shifting the time for lights off at 4 weeks after ischemia or sham procedure.

### Statistical analysis

The data were expressed as the means  $\pm$  SE. Statistical analysis of results was made by Student's *t*-test, and  $p < 0.05$  was considered statistically significant.

## RESULTS

(Figure 1) depicts the effect of retinal ischemia induced by increasing IOP to 120 mm Hg for 40 min on retinal function. Four weeks after treatment, a significant decrease in the scotopic ERG a- and b-wave and OP amplitude was observed in ischemic retinas as compared with retinas from eyes submitted to a sham procedure. No significant differences in ERG implicit times between non-ischemic and ischemic retinas were observed (data not shown). Representative scotopic ERG and OP traces from rat eyes submitted to ischemia or a sham procedure are also shown in Figure 1.

Representative photomicrographs of rat retinas submitted to a sham procedure or 40-min ischemia are shown in Figure 2. Four weeks after 40-min ischemia, the histological assessment with H&E staining showed typical histopathological features of ischemic damage in the retina, with clear alterations in retinal structure, and a significant reduction in the total retinal thickness, and the number of GCL cells. At 4 weeks after ischemia, a significant decrease in the number of Brn3a(+) cells was observed in flat-mounted retinas, as compared with the control group (Figure 3B). In order to analyze the influence of ischemia on mRGCs, the number of melanopsin(+) cells was analyzed by immunofluorescence. At 4 weeks post-treatment, no differences in the total number of melanopsin(+) cells were found between non-ischemic and ischemic retinas (Figure 3B). In order to further analyze the effect of ischemia on RGCs, Brn3a and melanopsin protein levels were assessed by Western blotting. As shown in Figure 4, a significant decrease in Brn3a levels was observed in ischemic retinas, whereas melanopsin levels did not differ between non-ischemic and ischemic retinas (Figure 4).

The active anterograde transport of RGC projections to the main retino-recipient targets in the brain was analyzed using CTB conjugated to Alexa 488 (green), injected into the vitreous from eyes submitted to a sham procedure, and CTB conjugated to Alexa 594 (red) injected in the vitreous from ischemic contralateral eyes, as shown in Figure 5. The projections from sham-treated eyes showed a strong CTB-staining (green) in the superficial layers of the SC, and in the LGN, whereas an almost complete absence of CTB-staining (red) was observed in the retino-recipient SC area and LGN which showed differences from the ischemic eye. No differences in the anterograde transport of CTB from the retina to the OPL and SCN were observed between sham-treated and ischemic eyes.

The PRL was examined in animals in which one eye was submitted to a sham procedure or ischemia, and the contralateral eye remained intact. When intense light (1200 lux) stimulated sham-treated or ischemic eyes, a similar magnitude of pupil contraction of the contralateral intact eye was observed (Figure 6). In contrast, when less intense light (120 lux) stimulated ischemic eyes, a significant decrease in the PLR of the intact eye

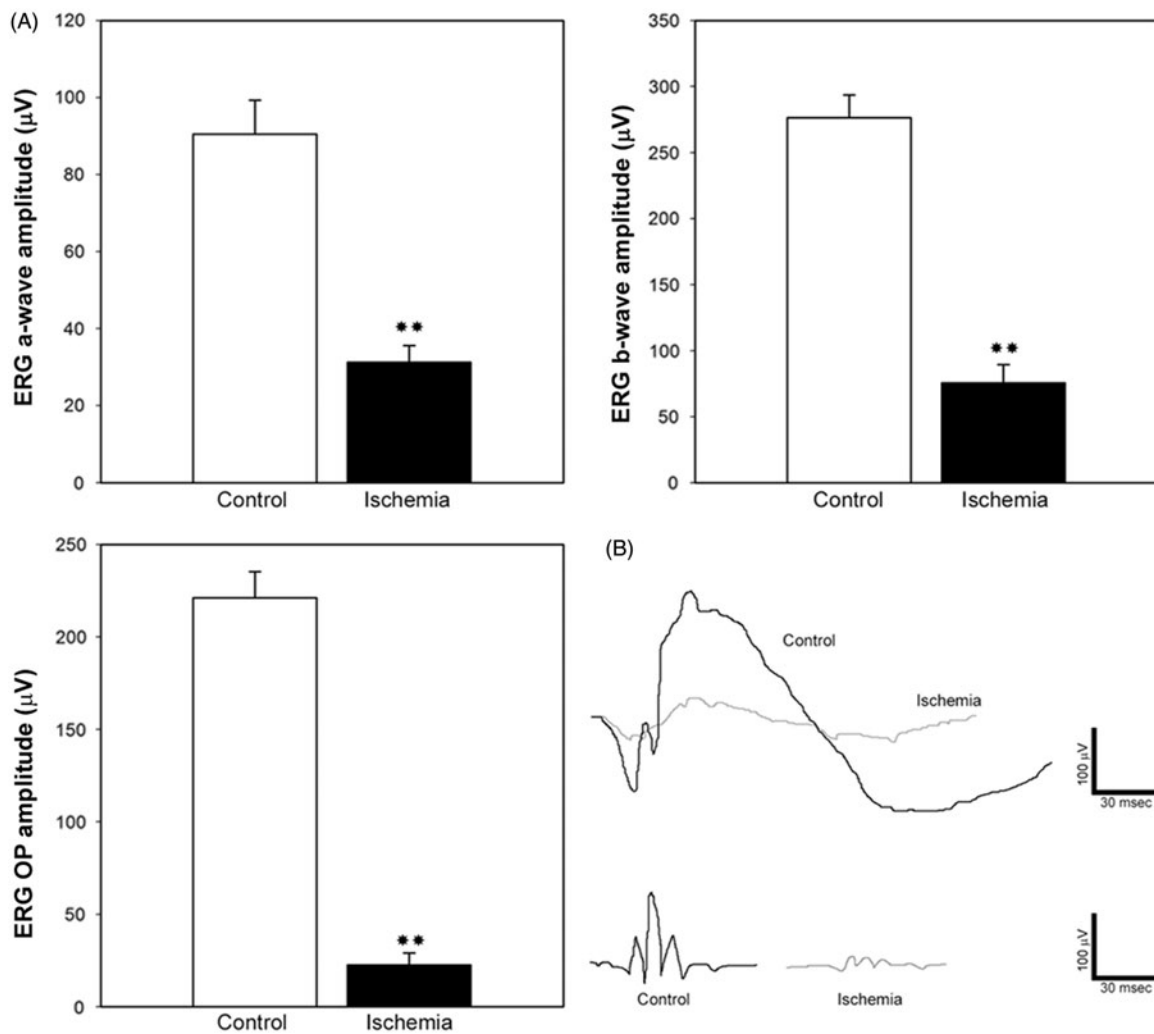


FIGURE 1. Effect of ischemia on retinal function. A: average amplitudes of scotopic ERG a-wave, b-wave, and OPs recorded at 4 weeks after ischemia. A significant decrease in ERG a-wave, b-wave, and OP amplitude was observed in animals submitted to 40-min ischemia, as compared with eyes submitted to a sham procedure. Data are mean  $\pm$  SE ( $n$ : 10 eyes/group). \*\* $p < 0.01$  versus sham-treated eyes, by Student's  $t$ -test. B: Representative scotopic ERG and OP traces of sham-treated and ischemic eyes.

was observed as compared with the pupil contraction of intact eyes contralateral to eyes submitted to a sham procedure.

The locomotor activity rhythm and the response to a phase shift in the L:D cycle were measured in animals bilaterally submitted to sham procedure or ischemia. The locomotor activity pattern in animals submitted to bilateral ischemia showed a normal rhythm of activity entrained to a L:D cycle (Figure 7). In addition, the phase angle of activity onset with respect to the time of lights off did not differ in animals bilaterally submitted to a sham procedure or ischemia. Moreover, the percentage of locomotor activity in the light and dark phase was similar in animals with bilateral ocular ischemia and in those submitted to a sham procedure in both eyes.

## DISCUSSION

The loss of RGCs and their axons is an important sign of retinal ischemia. The present results indicate a marked

preservation of a subtype of RGCs, mRGCs, which was functionally and structurally protected even after an extensive retinal damage such as that observed at 4 weeks after ischemia induced by increasing IOP to 120 mm Hg for 40 min.

In rodent models, functional (ERG) and conventional histological alterations progress over time after ischemia (Fernandez et al., 2009; Rosenbaum et al., 2001). In this report, we chose to wait 4 weeks after ischemia in order to maximize retinal functional and histological damage after an ischemic insult, and to discard the possibility of a transient protection (or a delayed death) of mRGC. In this vein, it was shown that RGC death induced by 45-min ischemia ends between 7 and 14 d post-ischemia (Lafuente et al., 2002).

In our experimental setting, retinal ischemia provoked a highly significant retinal dysfunction (as shown by a decrease in scotopic ERG a-wave, b-wave, and OP amplitude), and marked alterations of the retinal structure, which agreed with previous reports using similar

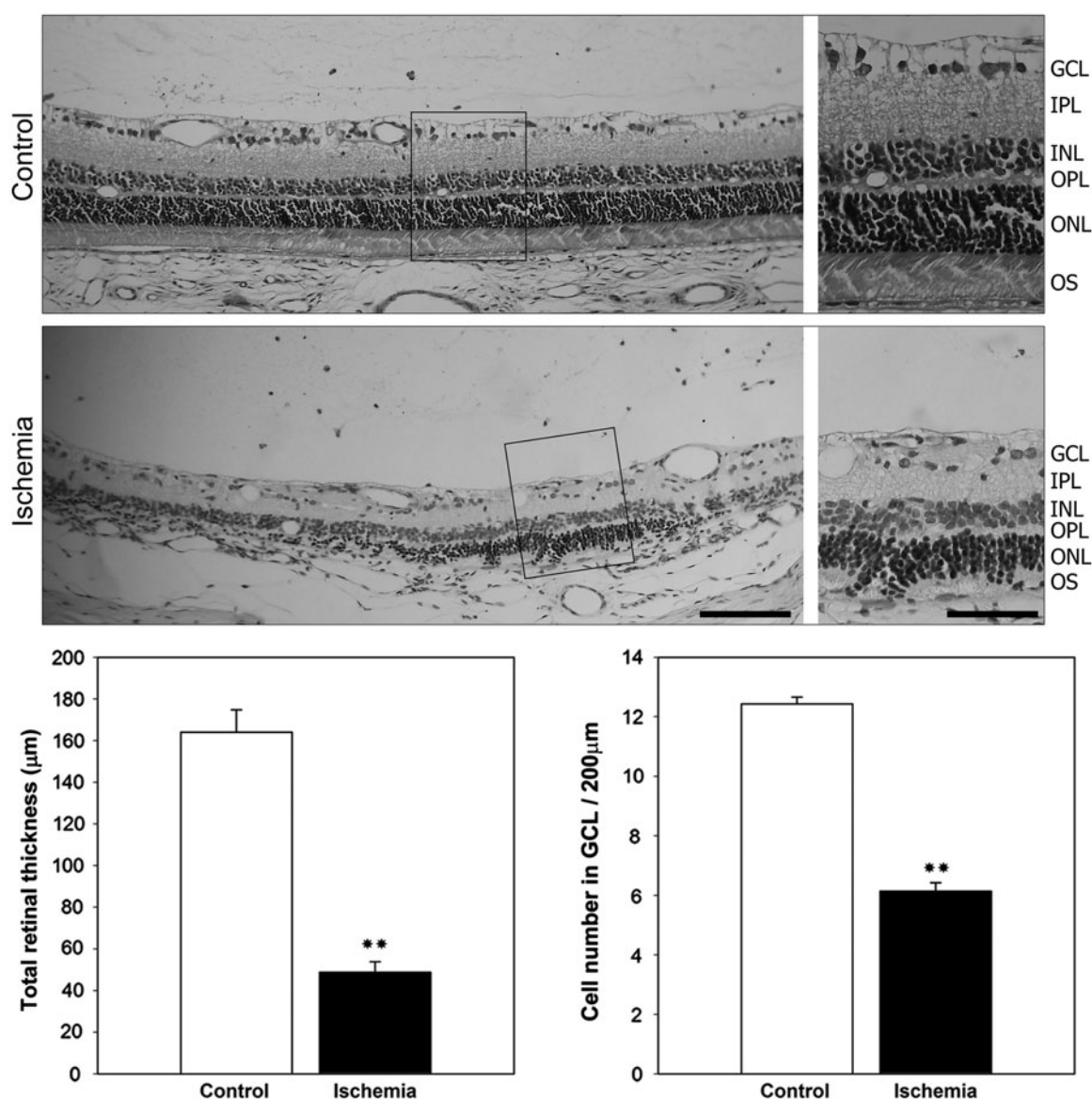


FIGURE 2. Effect of ischemia on retinal structure. Representative photomicrographs showing histological appearance of non-ischemic and ischemic retinas, at 4 weeks post-ischemia. Severe retinal damage is shown in the retina from eyes submitted to ischemia Scale bar = 100 μm and 50 μm (for details). GCL, ganglion cell layer; IPL, inner plexiform layer; INL, inner nuclear layer; ONL, outer nuclear layer; OS, outer segment of photoreceptors. Lower panel: Assessment of total retinal thickness and the number of GCL cells. Retinal ischemia induced a significant decrease in both parameters. Data are mean ± SEM ( $n = 5$  eyes per group), \*\* $p < 0.01$  versus sham-treated eyes, by Student's  $t$ -test.

experimental conditions (Dorfman et al., 2013; Fernandez et al., 2009; Kim et al., 2013).

Brn3a is a POU domain transcription factor specifically expressed in RGC nuclei (Nadal-Nicolás et al., 2009), and it was considered a marker for all RGCs. However, Jain et al. (2012) have demonstrated that the subpopulation of mRGCs do not express Brn3a. At 4 weeks post-ischemia, a significant decrease in Brn3a(+) cell number occurred, whereas no changes in melanopsin(+) cell number were evident. This result was supported by the assessment of Brn3a and melanopsin levels by Western blot which showed a significant decrease in Brn3a protein levels, whereas melanopsin levels remained unchanged in ischemic retinas. In agreement

with these results, it has been demonstrated an increase in the survival rate of mRGC as compared with those without melanopsin expression after optic nerve transection (Li et al., 2008; Robinson & Madison, 2004). Moreover, concomitantly with a significant decrease in the number of Brn3a(+) RGCs, the number of mRGC and melanopsin levels do not change at advanced stages of experimental diabetic retinopathy (Fernandez et al., 2013). Other evidences of mRGCs robustness are provided by studies on cell toxicity to kainic acid (Sakamoto et al., 2005) or N-Methyl-D-aspartate (DeParis et al., 2012) treatment. Furthermore, it was reported a relative sparing of mRGCs in two inherited mitochondrial disorders that cause blindness, i.e. Leber

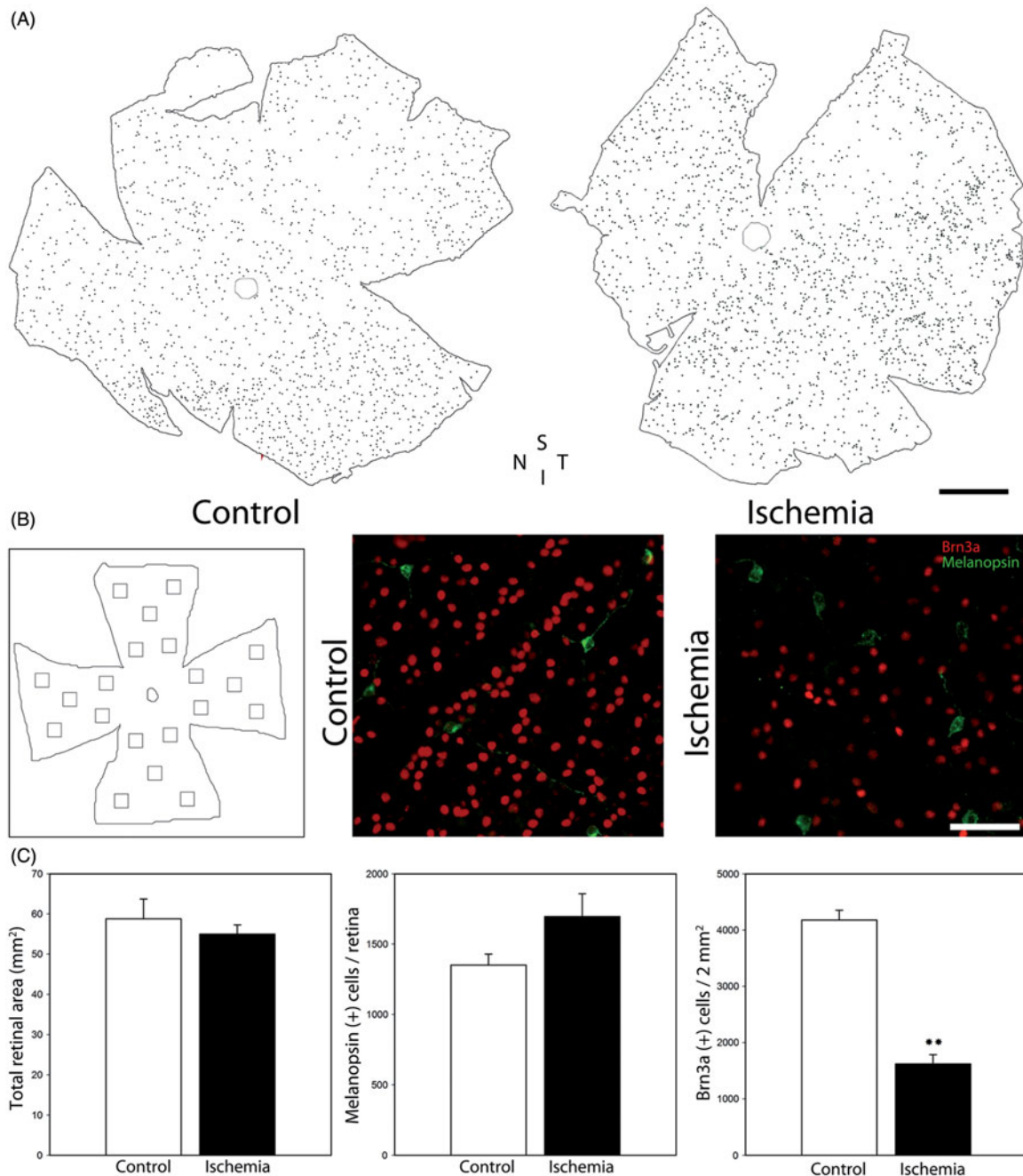


FIGURE 3. Effect of retinal ischemia on Brn3a(+) RGCs and melanopsin(+) RGCs. A: Representative diagrams showing the total number of melanopsin(+) cells per retina. N: nasal, T: temporal, S: superior, I: inferior. Panel B (left): Schematic diagram of a flat-mounted retina showing all the regions analyzed; Panel B (right): Shown are representative photomicrographs of double immunostaining for Brn3a and melanopsin cells in flat-mounted retinas from a sham-treated and an ischemic eye at 4 weeks after ischemia. Scale bar: A = 1000  $\mu$ m; B = 50  $\mu$ m. C: Quantification of total flat-mounted retinal area, Brn3a(+) cells, and melanopsin(+) cells. A significant decrease in the number of Brn3a(+) cells was observed in ischemic retinas, whereas melanopsin(+) RGC number and flat-mounted retinal area did not differ between groups. Data are mean  $\pm$  SEM ( $n = 5$  eyes per group), \*\* $p < 0.01$  versus sham-treated eyes, by Student's  $t$ -test.

hereditary optic neuropathy and dominant optic atrophy (La Morgia et al., 2010). In contradistinction, a progressive degeneration of mRGCs was demonstrated in an animal model of autosomal dominant retinitis pigmentosa (P23H rats) (Esquivia et al., 2013), and in Royal College of Surgeons dystrophic rats (Vugler et al., 2008). In addition, a reduction in mRGCs

(like other RGCs) number with ageing in human retinas (La Morgia et al., 2010), and animal models (Semo et al., 2003) was demonstrated. Glaucoma is the most common optic neuropathy characterized by an extensive loss of RGCs. The effect of glaucoma on mRGCs is still controversial. Two studies suggest that mRGCs may be spared in some animal models of chronic ocular



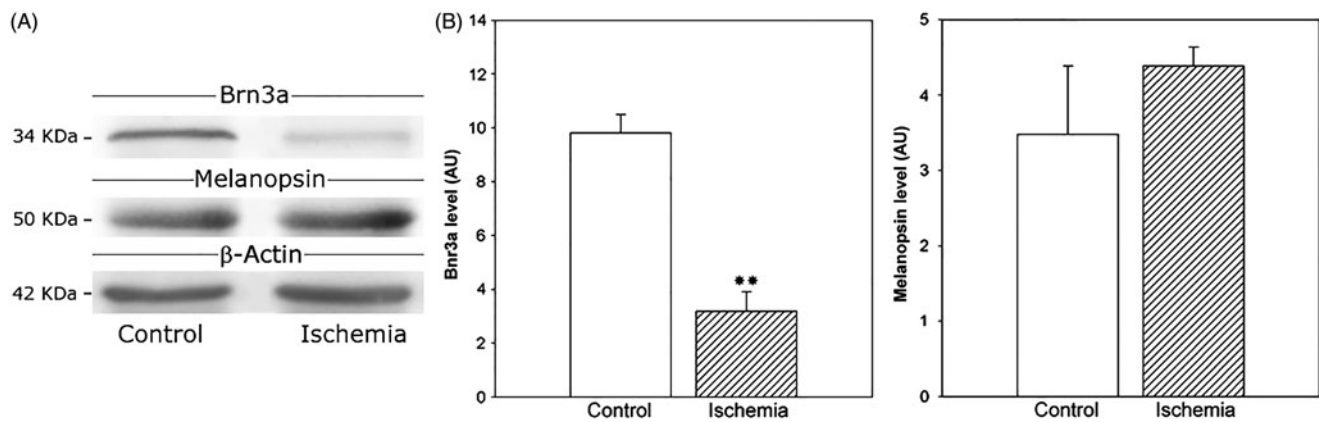


FIGURE 4. Effect of ischemia on Brn3a and melanopsin protein levels. (A) Shown are representative Western blots for the assessment of Brn3a and melanopsin levels in sham-treated or ischemic retinas at 4 weeks after ischemia. B: Densitometric analysis of all samples. Ischemia induced a significant decrease in Brn3a protein levels, whereas no changes in melanopsin levels were observed between groups. Data are the mean  $\pm$  SEM ( $n=5$  retinas/group); \*\* $p<0.01$  versus sham-treated eyes, by Student's  $t$ -test.

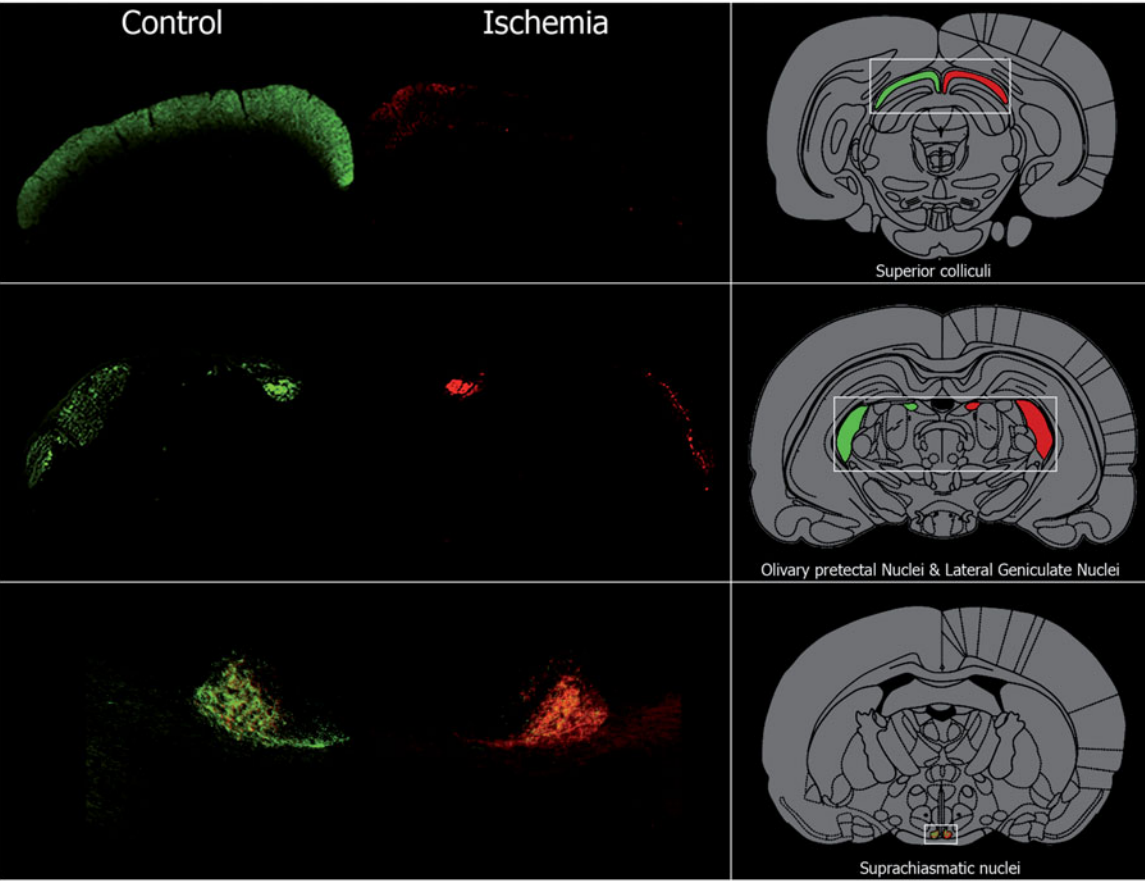


FIGURE 5. Anterograde transport from the retina to the SC, LGN, SCN, and OPN. CTB conjugated to Alexa 488 (left) was injected into the vitreous from eyes submitted to a sham procedure, and CTB conjugated to Alexa 594 (right) was injected in the vitreous from ischemic contralateral eyes. Upper panel: representative photomicrographs of coronal sections of the SC from an animal in which one eye was submitted to a sham procedure and the contralateral eye was submitted to ischemia. After 4 weeks of ischemia, a clear reduction of the retinal terminal density in the SC was observed in the retino-recipient area contralateral to an ischemic eye, as compared with the retino-recipient area contralateral to a sham-treated eye. Middle panel: no signs of alterations in the CTB-staining were observed in serial sections obtained at the OPN level between groups, while a decrease in the CTB staining in the LGN receiving input from an ischemic eye was found. Lower panel: CTB staining at the SCN level showing similar bilateral staining, and merge at both sides. The zone of interest is represented in the right panel. Shown are photomicrographs representative of 5 animals/group.



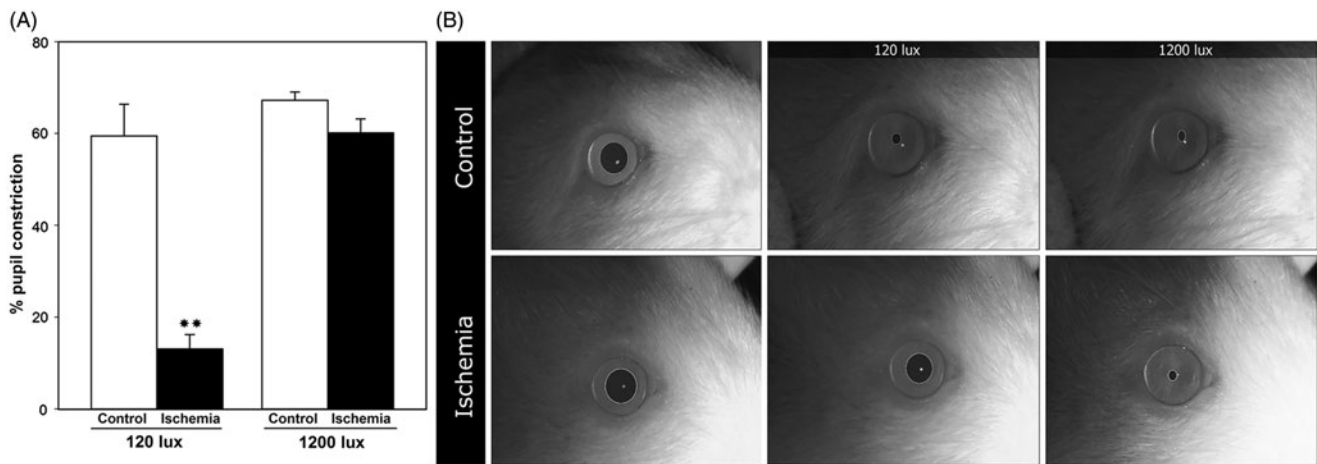


FIGURE 6. Assessment of the consensual PLR in animals in which one eye was submitted to a sham procedure or ischemia and the contralateral eye remained intact A: The pupil diameter (relative to the limbus diameter) was measured before and after a photic stimulus (white light, 120 or 1200 lux), and the percentage of pupil constriction was calculated. Retinal ischemia did not affect the consensual PLR when eyes were stimulated by intense light (1200 lux), but it decreased this parameter when eyes were stimulated by low intense light (120 lux). B: Representative images of the consensual PRL from eyes exposed to 120 lux or 1200 lux. Data are the mean  $\pm$  SEM ( $n=10$  animals/group). \*\* $p<0.01$  versus sham-treated eyes, by Student's  $t$ -test.

hypertension (Jakobs et al., 2005; Li et al., 2006), but other reports have shown the involvement of mRGCs as well as regular RGCs in experimental glaucomatous damage (de Zavalía et al., 2011; Drouyer et al., 2008; Wang et al., 2008). Taken together, these results suggest that the robustness of the mRGC could be not a general phenomenon, but it may depend on the nature of the injury.

With some exceptions, most of these reports assessed the preservation of mRGC by Western blot analysis and/or immunohistochemistry, but relatively few studies have investigated the preservation of the functional capacity of the non-image-forming visual system in retinal disorders. Many lines of evidence support that the non-image-forming visual pathway is disturbed or impaired in experimental glaucoma (de Zavalía et al., 2011; Drouyer et al., 2008; Wang et al., 2008). In addition, abnormal circadian rhythm of melatonin secretion and of light-induced melatonin suppression was described in glaucoma patients (Pérez-Rico et al., 2010). Moreover, locomotor activity rhythm, sleep parameters (Lanzani et al., 2012), and the PLR are also affected in glaucoma patients (Kalaboukhova et al., 2007). Although retinal ischemia has been involved in glaucomatous damage (Osborne et al., 1999; Quaranta et al., 2013), the present results showed that mRGC related functions remained unchanged at 4 weeks after retinal ischemia.

In rodents, most RGC axons project contralaterally to the SC and LGN (Kondo et al., 1993). Retinal ischemia induced an almost complete deficit of CTB anterograde transport to the contralateral SC and LGN, whereas no evident changes in CTB anterograde transport from ischemic retinas to the SCN and OPN were evident. Moreover, using green and red anterograde tracers, a similar staining for both colors in each SCN

was observed, which is consistent with previous reports showing bilateral projections to the SCN from mRGCs from each eye (Gooley et al., 2003). Since the majority of SCN and OPN-projecting RGCs are melanopsin-immuno-positive (Hattar et al., 2006), these results support a preservation of mRGC axons after ischemic damage. In addition to the soma and axon protection, the present results support that the mRGC functionality was also preserved in ischemic retinas. Pupil responses differ as a function of light intensity and wavelength, and selected stimulus conditions can produce pupil responses that reflect phototransduction primarily mediated by rods, cones, or melanopsin. In that context, it is accepted that responses driven by melanopsin occur at higher illumination levels, and at lower light intensity, cones and rods would be involved in PRL changes (Grozdanic et al., 2007; Lucas et al., 2003). As shown herein, when eyes were stimulated with high intense light, the consensual PLR to ischemic eyes was completely preserved, which is compatible with the preservation of the CTB anterograde transport from ischemic retinas to the OPN which projects to the Edinger-Westphal nucleus and controls PLR (Young & Lund, 1998). In contrast, at a low-intensity light, ischemia induced a significant decrease in the consensual PRL, which was in agreement with histological results and with a photoreceptor dysfunction shown by the decrease in the ERG induced by ischemia.

In order to analyze the functional communication between mRGCs and the mammalian circadian clock, we recorded general activity patterns of animals in which both eyes were submitted to a sham procedure or ischemia. Animals with ocular bilateral ischemia exhibited circadian rhythms under a light-dark cycle, and a re-entrainment rate of locomotor activity rhythm after a phase delay of the L:D cycle which were similar to

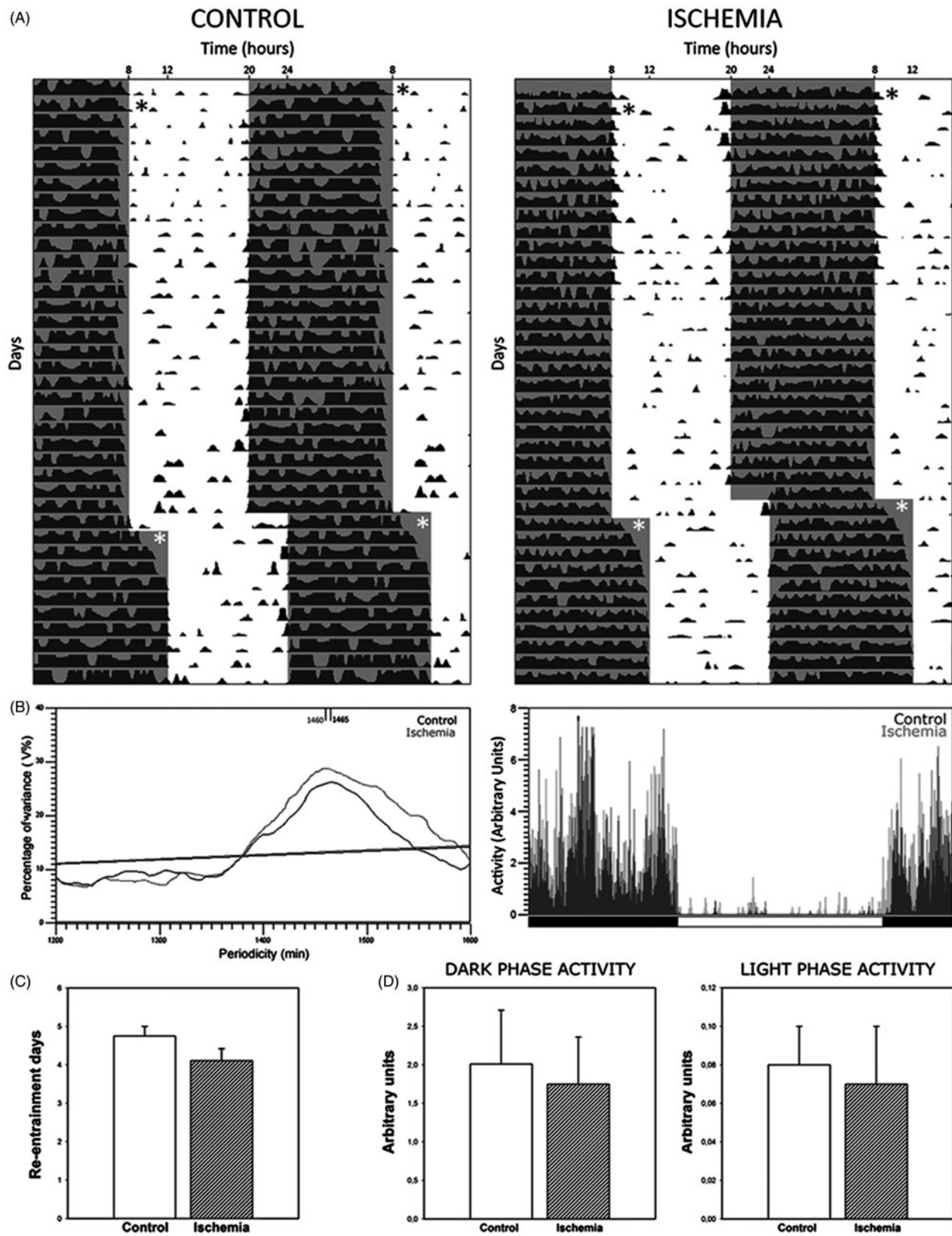


FIGURE 7. Locomotor activity rhythm from animals bilaterally submitted to sham procedure or ischemia. A: Representative double-plotted actograms after sham or ischemia (black asterisks) from animals under a normal L:D cycle. A 4 h phase delay in the L:D cycle was applied (white asterisks) and the period needed for re-entrainment was evaluated. B: Periodogram from sham-treated animals (black trace) were similar to ischemic animals (grey trace). Representative waveforms from sham-treated (black) or ischemic animals (grey). There were no differences in light or dark phase activity between groups (quantified in D). C: Time for re-entrainment after a 4 h-phase delay in the L:D cycle in sham-treated or ischemic animals. No significant differences were observed between groups. Data are the mean  $\pm$  SEM ( $n = 5$  animals/group).

those observed in animals submitted to a sham procedure in both eyes. In addition, a normal phase angle for the start of their nocturnal locomotion was also observed in animals with bilateral retinal ischemia.

The present results support the concept that mRGCs are different from “traditional” RGCs and that they may have an intrinsic strength to survive after retinal ischemia. Some mechanisms have been involved in mRGC robustness, particularly neuropeptide pituitary adenylate cyclase activating polypeptide (PACAP), which is expressed in mRGCs (Hannibal et al., 2002) and phosphatidylinositol-3 kinase (PI3K/Akt) (Li et al., 2008), but there are also evidence which argues against these explanations (DeParis et al., 2012; Perganta et al., 2013). Although it seems likely that different mechanisms could account for specific protection depending on the nature of the injury, identifying the mechanisms which confer to mRGCs an increased survival ability, might pave the way for finding novel therapeutic agents able to protect all RGCs. The circadian clock mechanism and the entrainment pathway represent extremely robust processes that have been fairly conserved in evolutionary terms (reviewed by Golombek & Rosenstein, 2010). Considering the key role of mRGCs in the circadian physiology, it seems likely that a long-lasting evolutionary pressure conserved this photoreceptive system, providing them with an intrinsic strength to survive in front of different challenges.

Although we still do not know whether the neural circuit within the retina, the unique functionalities of this group of cells, a protection achieved by melanopsin itself, or a combinations of these characteristics contributes to the survival after ischemic injury, based on this experimental study, it can be presumed that despite their low vision, patients with retinal ischemia such as those with central retinal artery or ophthalmic artery occlusion, could retain the neuronal substrate and the functionality of the non-image forming visual system, thus avoiding consequences of circadian misalignment. Further studies are warranted to clarify the involvement of mRGCs in human retinal ischemia.

## DECLARATION OF INTEREST

This research was supported by grants from the Agencia Nacional de Promoción Científica y Tecnológica [PICT 1623]; The University of Buenos Aires [20020100100678]; Consejo Nacional de Investigaciones Científicas y Técnicas [PIP 1911], Argentina. The funding organizations have no role in the design or conduct of this research. The authors report no conflicts of interest.

## REFERENCES

- Berson DM, Dunn FA, Takao M. (2002). Phototransduction by retinal ganglion cells that set the circadian clock. *Science*. 295:1070–3.
- Berson DM. (2003). Strange vision: Ganglion cells as circadian photoreceptors. *Trends Neurosci*. 26:314–20.
- Bonne C, Muller A, Villain M. (1998). Free radicals in retinal ischemia. *Gen Pharmacol*. 30:275–80.
- Bresnick GH, De Venecia G, Myers FL, et al. (1975). Retinal ischemia in diabetic retinopathy. *Arch Ophthalmol*. 93:1300–10.
- Chidlow G, Osborne NN. (2003). Rat retinal ganglion cell loss caused by kainate, NMDA and ischemia correlates with a reduction in mRNA and protein of Thy-1 and neurofilament light. *Brain Res*. 963:298–306.
- de Zavalía N, Plano SA, Fernandez DC, et al. (2011). Effect of experimental glaucoma on the non-image forming visual system. *J Neurochem*. 117:904–14.
- DeParis S, Caprara C, Grimm C. (2012). Intrinsically photosensitive retinal ganglion cells are resistant to N-methyl-D-aspartic acid excitotoxicity. *Mol Vis*. 18:2814–27.
- Dorfman D, Fernandez DC, Chianelli M, et al. (2013). Post-ischemic environmental enrichment protects the retina from ischemic damage in adult rats. *Exp Neurol*. 240:146–56.
- Drouyer E, Dkhis-Benyahya O, Chiquet C, et al. (2008). Glaucoma alters the circadian timing system. *PLoS One*. 3:e3931.
- Esquivá G, Lax P, Cuenca N. (2013). Impairment of intrinsically photosensitive retinal ganglion cells associated with late stages of retinal degeneration. *Invest Ophthalmol Vis Sci*. 54:4605–18.
- Fernandez DC, Chianelli MS, Rosenstein RE. (2009). Involvement of glutamate in retinal protection against ischemia/reperfusion damage induced by post-conditioning. *J Neurochem*. 111:488–98.
- Fernandez DC, Sande PH, de Zavalía N, et al. (2013). Effect of experimental diabetic retinopathy on the non-image-forming visual system. *Chronobiol Int*. 30:583–97.
- Golombek DA, Rosenstein RE. (2010). Physiology of circadian entrainment. *Physiol Rev*. 90:1063–102.
- Gooley JJ, Lu J, Chou TC, et al. (2001). Melanopsin in cells of origin of the retinohypothalamic tract. *Nat Neurosci*. 4:1165.
- Gooley JJ, Lu J, Fischer D, Saper CB. (2003). A broad role for melanopsin in nonvisual photoreception. *J Neurosci*. 23:7093–106.
- Grozdanic SD, Matic M, Sakaguchi DS, Kardon RH. (2007). Evaluation of retinal status using chromatic pupil light reflex activity in healthy and diseased canine eyes. *Invest Ophthalmol Vis Sci*. 48:5178–83.
- Guido ME, Garbarino-Pico E, Contin MA, et al. (2010). Inner retinal circadian clocks and non-visual photoreceptors: Novel players in the circadian system. *Progr Neurobiol*. 92:484–504.
- Hankins MW, Peirson SN, Foster RG. (2008). Melanopsin: An exciting photopigment. *Trends Neurosci*. 31:27–36.
- Hannibal J, Hindersson P, Knudsen SM, et al. (2002). The photopigment melanopsin is exclusively present in pituitary adenylate cyclase-activating polypeptide-containing retinal ganglion cells of the retinohypothalamic tract. *J Neurosci*. 22:RC191.
- Hattar S, Kumar M, Park A, et al. (2006). Central projections of melanopsin-expressing retinal ganglion cells in the mouse. *J Comp Neurol*. 497:326–49.
- Hattar S, Liao HW, Takao M, et al. (2002). Melanopsin-containing retinal ganglion cells: Architecture, projections, and intrinsic photosensitivity. *Science*. 295:1065–70.
- Hattar S, Lucas RJ, Mrosovsky N, et al. (2003). Melanopsin and rod-cone photoreceptive systems account for all major accessory visual functions in mice. *Nature*. 424:76–81.
- Jain V, Ravindran E, Dhingra NK. (2012). Differential expression of Brn3 transcription factors in intrinsically photosensitive retinal ganglion cells in mouse. *J Comp Neurol*. 520:742–55.
- Jakobs TC, Libby RT, Ben Y, et al. (2005). Retinal ganglion cell degeneration is topological but not cell type specific in DBA/2J mice. *J Cell Biol*. 171:313–25.



- Kalaboukhova L, Fridhammar V, Lindblom B. (2007). Relative afferent pupillary defect in glaucoma: A pupillometric study. *Acta Ophthalmol Scand.* 85:519–25.
- Kim BJ, Braun TA, Wordinger RJ, Clark AF. (2013). Progressive morphological changes and impaired retinal function associated with temporal regulation of gene expression after retinal ischemia/reperfusion injury in mice. *Mol Neurodegener.* 8:21.
- Kondo Y, Takada M, Honda Y, Mizuno N. (1993). Bilateral projections of single retinal ganglion cells to the lateral geniculate nuclei and superior colliculi in the albino rat. *Brain Res.* 608:204–15.
- Kuehn MH, Fingert JH, Kwon YH. (2005). Retinal ganglion cell death in glaucoma: Mechanisms and neuroprotective strategies. *Ophthalmol Clin North Am.* 18:383–95.
- La Morgia C, Ross-Cisneros FN, Sadun AA, et al. (2010). Melanopsin retinal ganglion cells are resistant to neurodegeneration in mitochondrial optic neuropathies. *Brain.* 133: 2426–38.
- Lafuente MP1, Villegas-Pérez MP, Sellés-Navarro I, et al. (2002). Retinal ganglion cell death after acute retinal ischemia is an ongoing process whose severity and duration depends on the duration of the insult. *Neuroscience.* 109:157–68.
- Lanzani MF, de Zavalía N, Fontana H, et al. (2012). Alterations of locomotor activity rhythm and sleep parameters in patients with advanced glaucoma. *Chronobiol Int.* 29:911–9.
- Li RS, Chen BY, Tay DK, et al. (2006). Melanopsin-expressing retinal ganglion cells are more injury-resistant in a chronic ocular hypertension model. *Invest Ophthalmol Vis Sci.* 47: 2951–8.
- Li SY, Yau SY, Chen BY, et al. (2008). Enhanced survival of melanopsin-expressing retinal ganglion cells after injury is associated with the PI3 K/Akt pathway. *Cell Mol Neurobiol.* 28: 1095–107.
- Liu Y, Liu XJ, Sun D. (2009). Ion transporters and ischemic mitochondrial dysfunction. *Cell Adh Migr.* 3:94–8.
- Lowry OH, Rosebrough NJ, Farr AL, Randall RJ. (1951). Protein measurement with the Folin Phenol reagent. *J Biol Chem.* 193: 265–75.
- Lucas RJ, Douglas RH, Foster RG. (2001). Characterization of an ocular photopigment capable of driving pupillary constriction in mice. *Nat Neurosci.* 4:621–6.
- Lucas RJ, Hattar S, Takao M, et al. (2003). Diminished pupillary light reflex at high irradiances in melanopsin-knockout mice. *Science.* 299:245–7.
- Nadal-Nicolás FM, Jiménez-López M, Sobrado-Calvo P, et al. (2009). Brn3a as a marker of retinal ganglion cells: Qualitative and quantitative time course studies in naive and optic nerve-injured retinas. *Invest Ophthalmol Vis Sci.* 50:3860–8.
- Osborne NN, Casson RJ, Wood JP, et al. (2004). Retinal ischemia: Mechanisms of damage and potential therapeutic strategies. *Progr Retin Eye Res.* 23:91–147.
- Osborne NN, Chidlow G, Nash MS, Wood JP. (1999). The potential of neuroprotection in glaucoma treatment. *Curr Opin Ophthalmol.* 10:82–92.
- Panda S, Provencio I, Tu DC, et al. (2003). Melanopsin is required for non-image-forming photic responses in blind mice. *Science.* 301:525–7.
- Paxinos G, Watson C. (1997). *The rat brain in stereotaxic coordinates.* Amsterdam: Elsevier.
- Pérez-Rico C, de la Villa P, Arribas-Gómez I, Blanco R. (2010). Evaluation of functional integrity of the retinohypothalamic tract in advanced glaucoma using multifocal electroretinography and light-induced melatonin suppression. *Exp Eye Res.* 91: 578–83.
- Perganta G, Barnard AR, Katti C, et al. (2013). Non-image-forming light driven functions are preserved in a mouse model of autosomal dominant optic atrophy. *PLoS One.* 8:e56350.
- Portaluppi F, Smolensky MH, Touitou Y. (2010). Ethics and methods for biological rhythm research on animals and human beings. *Chronobiol Int.* 27:1911–29.
- Provencio I, Rollag MD, Castrucci AM. (2002). Photoreceptive net in the mammalian retina. This mesh of cells may explain how some blind mice can still tell day from night. *Nature.* 415:493.
- Quaranta L, Katsanos A, Russo A, Riva I. (2013). 24-Hour intraocular pressure and ocular perfusion pressure in glaucoma. *Surv Ophthalmol.* 58:26–41.
- Robinson GA, Madison RD. (2004). Axotomized mouse retinal ganglion cells containing melanopsin show enhanced survival, but not enhanced axon regrowth into a peripheral nerve graft. *Vision Res.* 44:2667–74.
- Rosenbaum DM, Rosenbaum PS, Singh M, et al. (2001). Functional and morphologic comparison of two methods to produce transient retinal ischemia in the rat. *J Neuroophthalmol.* 21: 62–8.
- Sakamoto K, Liu C, Kasamatsu M, et al. (2005). Dopamine regulates melanopsin mRNA expression in intrinsically photosensitive retinal ganglion cells. *Eur J Neurosci.* 22:3129–36.
- Semo M, Lupi D, Peirson SN, et al. (2003). Light-induced c-fos in melanopsin retinal ganglion cells of young and aged rodless/coneless (rd/rd cl) mice. *Eur J Neurosci.* 18:3007–17.
- Szydlowska K, Tymianski M. (2010). Calcium, ischemia and excitotoxicity. *Cell Calcium.* 47:122–9.
- Vugler AA, Semo M, Joseph A, Jeffery G. (2008). Survival and remodeling of melanopsin cells during retinal dystrophy. *Vis Neurosci.* 25:125–38.
- Wang HZ, Lu QJ, Wang NL, et al. (2008). Loss of melanopsin containing retinal ganglion cells in a rat glaucoma model. *Chin Med J (Engl).* 121:1015–9.
- Young MJ, Lund RD. (1998). The retinal ganglion cells that drive the pupilloconstrictor response in rats. *Brain Res.* 787:191–202.